Adsorption of a hard sphere fluid in a slitlike pore filled with a disordered matrix by the inhomogeneous replica Ornstein-Zernike equations

Andrij Kovalenko
Institute of Condensed Matter Physics, Ukrainian National Academy of Sciences, Lviv 11, Ukraine

Stefan Sokołowski
Department for the Modelling of Physico-Chemical Processes, Faculty of Chemistry, MSC University, 200-31 Lublin, Poland

Douglas Henderson
Department of Chemistry and Biochemistry, Brigham Young University, Provo, Utah 84602

Orest Pizio
Instituto de Química de la UNAM, Circuito Exterior, Coyoacán 04510, México Distrito Federal, Mexico
(Received 23 July 1997)

The density distribution and pair distribution functions for a fluid adsorbed in a slitlike pore filled with a quenched disordered hard sphere fluid are studied using the *inhomogeneous* replica Ornstein-Zernike equations with the *inhomogeneous* Percus-Yevick (PY) and hypernetted chain (HNC) approximations. The one and two particle functions are related via the Born-Green-Yvon equation. For comparison, grand canonical Monte Carlo simulation data are obtained. The agreement of the integral equation results with the simulation data is good. In particular, we find ''layering'' in the density profiles near the pore boundaries. As the width of the pore is decreased, these layers are ''squeezed'' out. The pair functions are also described satisfactorily by the integral equations. The HNC results tend to be greater than the PY results near contact. [S1063-651X(98)04401-8]

PACS number(s): 61.25.−f, 61.20.−p, 61.43.Dq, 68.45.Da

I. INTRODUCTION

Recently, the problem of describing the structure and thermodynamics of quenched-annealed (QA) mixtures has received considerable experimental and theoretical interest. Such mixtures are comprised by a fluid component equilibrated in a matrix component. The matrix consists of particles quenched in a disordered configuration obtained from an equilibrium ensemble equilibrated in the absence of the annealed species.

The experimental studies [1–4] have focused on phase transitions in these systems. In particular, a remarkable difference has been observed for the liquid-vapor and of the liquid-liquid coexistence curves for the quenched-annealed and purely annealed mixtures. Also, computer simulations have been applied to QA fluids. Even though the models are simplified, these computer studies describe the important features of the phase diagram, its dependence on the interparticle interactions, and have provided a detailed description of the structural properties in terms of the distribution functions.

Theoretical investigations of adsorption of fluids in quenched disordered and random matrices commence from the adaptation of the methods of liquid-state statistical mechanics for usual mixtures. Random matrices are those in which particles do not interact between themselves (ideal gas) but interact with the fluid component.

Madden and Glandt [5,6] have derived cluster expansions for the distribution functions and thermodynamic properties for the systems in question and have obtained a set of Ornstein-Zernike–(OZ-) like integral equations for the relevant correlation functions. More recently, Given and Stell [7–9] have extended the replica method for the adsorption of homogeneous fluids in quenched disordered and random matrices. The replica Ornstein-Zernike (ROZ) equations represent one of their important results. Some models for QA systems have been analyzed in subsequent theoretical studies and computer simulations [10–17]. The adequacy of the closure approximations for the ROZ equations has been studied and reliable adsorption isotherms for simple models have been obtained. Still there remains room for further theoretical progress. In particular, the virial route for thermodynamic properties of quenched-annealed mixtures is not sufficiently well probed, in spite of much effort [7,13,18].

The majority of the aforementioned studies have been restricted to a hard sphere fluid adsorbed either in a hard sphere disordered matrix or in random matrices; see, e.g., [14,15,17]. In some studies that focused on the liquid-vapor transition, the Lennard-Jones interaction between the fluid particles has been used [16,19]. A lowering of the critical temperature of the adsorbed fluid with increasing matrix density has been observed. However, the detailed shape of the coexistence curve depends crucially on the approximations involved [19]. Very few attempts to consider quenched-annealed systems with Coulomb forces have been undertaken [20,21]. We have initiated a study of associative fluids in disordered matrices employing the associative extension of ROZ equations [22–25]. The use of differing interparticle interactions in models for QA mixtures has contributed to our knowledge of these systems.

However, in contrast to previous studies, in this work our focus is *inhomogeneous* quenched-annealed (IQA) fluids. This problem is of practical interest for gel-exclusion chromatography in separation science. Also, the study of adsorp-

 © 1998 The American Physical Society

tion of fluids in pores filled with a quenched component has relevance to the extraction methodology from porous rocks. Further, it is of importance for the study of fluids adsorbed in clays with quenched disordered pillars.

Actually, even in the construction of the theory for homogeneous QA mixtures, some background from the study of inhomogeneous fluids is needed [13,18]. The problem of IQA fluids was stated formally first in [26]. The inhomogeneous replica Ornstein-Zernike equations, complemented by either the Born-Green-Yvon (BGY), or the Lovett-Mou-Buff-Wertheim (LMBW) equation for the density profiles, were proposed to study the adsorption of a fluid near a plane boundary of a disordered matrix that has been assumed uniform in a half-space.

However, to our knowledge, no numerical solution for an IQA fluid was presented until our very recent communication [27], dedicated to the adsorption of a hard sphere fluid in a slitlike pore filled with a quenched disordered matrix. The format of that paper did not permit a detailed discussion of the results. Moreover, that numerical solution of the ROZ equations for IQA fluids was not compared with computer simulation results. Our focus in this more extended paper is to present some results that follow from the solution of the ROZ equations and compare them with grand canonical Monte Carlo (GCMC) simulation data. For the sake of simplicity, we will restrict ourselves to the same simple model used previously. Thus, we consider a hard sphere fluid adsorbed in a slitlike pore in which a disordered quenched matrix of hard spheres has been prepared in advance.

The structure of the paper is as follows. We begin with the description of the model and follow with a discussion of the theoretical method. The numerical procedure and the methodology of computer simulations are given in the final part of Sec. II. In Sec. III we present the results that are obtained. Finally, a summarizing discussion is given in Sec. IV.

II. A MODEL FOR INHOMOGENEOUS QUENCHED-ANNEALED SYSTEM AND THEORETICAL PROCEDURE

The model proposed in [27] describes an IQA fluid in a slitlike pore. We assume that a fluid consisting of particles of species m has been adsorbed in a slitlike pore of the width H. The fluid m is the matrix component of the QA mixture. The pore walls are chosen to be normal to the z axis and the pore is centered at $z=0$. The matrix is assumed to be in equilibrium with its bulk counterpart at the chemical potential μ_m. The structural aspects of the matrix state are characterized by the density profile $\rho_m(z)$ and by the inhomogeneous pair correlation function $h_{mm}(1,2)$. We assume that, due to external factors, the structure of the matrix species becomes quenched at a state determined by μ_m. Thus, a confined porous medium (matrix-filled slitlike pore) has been formed.

Now, we turn our attention to a subsequent physical adsorption of another fluid, belonging to the species f, in the matrix-filled pore. The thermodynamic state of the fluid f outside the matrix-filled pore is determined by the chemical potential μ_f. In the equilibrium state, the adsorbed fluid f has the one particle density distribution $\rho_f(z)$. In contrast to the case of a fluid adsorbed in a matrix-free pore, the one-particle density functional depends on the chemical potential of the matrix species, $\rho_f(z;\mu_m)$. The pair distribution of the f particles may be characterized by the inhomogeneous correlation function $h_{ff}(1,2)$. Similar to previous studies [7–9], the matrix and fluid species in what follows bear subscripts 0 and 1, respectively. We assume the simplest form for the interactions between particles and between the particles and pore walls, choosing both species as hard spheres of diameter σ_i, $i=0,1$,

$$U_{ij}(r)=\begin{cases}\infty, & r<\sigma_{ij}\\ 0, & r>\sigma_{ij},\end{cases}\quad U_i(z)=\begin{cases}\infty, & z<0.5|H-\sigma_i|\\ 0 & \text{otherwise,}\end{cases} \tag{1}$$

where i,j are species indices.

We begin with the presentation of theoretical tools for the determination of the matrix structure. In contrast to the usual (annealed) mixtures (where the correlations of all involved components are coupled), the matrix structural characteristics for QA mixtures are the input. Usually, for homogeneous matrices, the structure is obtained by solving the Ornstein-Zernike equation employing any of standard liquid-state closures; see, e.g., [14,15]. As mentioned above, we choose the matrix structure to correspond to the equilibrium grand canonical ensemble for matrix particles in a pore. A computer simulated structure may be used for this purpose. However, to be consistent with the following procedure for the fluid-fluid and the fluid-matrix correlations, in this work we obtain the structure of a quenched inhomogeneous matrix, using the inhomogeneous, or second order, Ornstein-Zernike (OZ2) equation, which reads

$$h_{00}(1,2)-c_{00}(1,2)=\int d3\rho_0(z_3)c_{00}(1,3)h_{00}(3,2), \tag{2}$$

supplemented by the LMBW equation for the density profile (DP)

$$\frac{\partial \ln\rho_0(z_1)}{\partial z_1}+\frac{\partial\beta U(z_1)}{\partial z_1}=\int d2c_{00}(1,2)\,\frac{\partial\rho_0(z_2)}{\partial z_2} \tag{3}$$

and the second order Percus-Yevick (PY2) closure

$$y_{00}(1,2)=1+h_{00}(1,2)-c_{00}(1,2). \tag{4}$$

In Eq. (4), $y_{00}(1,2)$ is the inhomogeneous cavity distribution function. The solution of the problem, comprising Eqs. (2)–(4), yields $\rho_0(z)$ and $h_{00}(1,2)$, such that the one-particle cavity distribution function $y_0(z)$, $y_0(z)=\rho_0(z)\exp[\beta U(z)]$, tends to its limiting value outside the pore region. This value is determined by the configurational part of the chemical potential for the matrix species, $y_0(z\to\pm\infty)=\exp(\beta\mu_0)$.

Let us proceed with the inhomogeneous replica Ornstein-Zernike equations that represent the essence of the theoretical procedure. They are given as follows [26]:

$$h_{10}(1,2)-c_{10}(1,2)=\int d3\rho_0(z_3)c_{10}(1,3)h_{00}(3,2)+\int d3\rho_1(z_3)c_{c,11}(1,3)h_{10}(3,2),$$

$$h_{01}(1,2)-c_{01}(1,2)=\int d3\rho_0(z_3)c_{00}(1,3)h_{01}(3,2)+\int d3\rho_1(z_3)c_{01}(1,3)h_{c,11}(3,2),$$

$$h_{11}(1,2)-c_{11}(1,2)=\int d3\rho_0(z_3)c_{10}(1,3)h_{01}(3,2)+\int d3\rho_1(z_3)c_{c,11}(1,3)h_{11}(3,2)+\int d3\rho_1(z_3)c_{b,11}(1,3)h_{c,11}(3,2),$$

$$h_{c,11}(1,2)-c_{c,11}(1,2)=\int d3\rho_1(z_3)c_{c,11}(1,3)h_{c,11}(3,2). \tag{5}$$

The fluid-fluid pair (h) and direct (c) correlation functions consist of the blocking and connected part, $\varphi_{11}(1,2)=\varphi_{b,11}(1,2)+\varphi_{c,11}(1,2)$, where the function φ stands for h or c, as appropriate. The blocking part of the inhomogeneous fluid-fluid pair correlation function corresponds to the subset of graphs constructed from the Mayer functions of the interparticle interactions such that all paths between the two root points pass through at least one matrix field point [26], similar to bulk QA fluids [7–9,14]. However, for our model, the root and field points are weighted by the Boltzmann factors of the relevant external field.

We apply the BGY equation as the relation that couples the local densities (density profiles) with the inhomogeneous pair correlation functions. The BGY equation reads [26]

$$\frac{\partial \ln \rho_1(z_1)}{\partial z_1}+\beta\frac{\partial w(z_1)}{\partial z_1}=-\beta\int d2\rho_1(z_2)g_{11}(1,2)\times\frac{\partial U_{11}(12)}{\partial z_2}, \tag{6}$$

where $g_{11}(1,2)=1+h_{11}(1,2)$, and the effective one-body potential $w(z)$ satisfies the relation

$$\frac{\partial w(z_1)}{\partial z_1}=\frac{\partial U(z_1)}{\partial z_1}+\int d2\rho_0(z_2)g_{10}(1,2)\frac{\partial U_{10}(12)}{\partial z_2}. \tag{7}$$

and where $g_{10}(1,2)=1+h_{10}(1,2)$. In fact, one could use the LMBW equation for the density profiles instead of the BGY equation. The former also has been derived in [26]. However, we find the application of the LMBW equation less clear methodologically; it requires an additional approximation for an ''auxilary'' direct correlation function of the fluid-matrix correlations. See [26] for a more detailed discussion; here we only comment that if one uses a representation of the IQA system in the form of its replicated analog, then using the BGY equation involves taking straightforward derivatives with respect to the external field whereas the LMBW equation formally requires derivatives with respect to the pair interaction potential of particles belonging to noninteracting replicas of the original fluid.

Finally, the closure relations for the inhomogeneous pair functions must be chosen. The detailed analysis of Stell and Given [7–9] (see also Ref. [14] for more details) has shown that the hypernetted chain closure is consistent with the ROZ equations for the adsorption of fluids in homogeneous disordered matrices while the PY closure belongs to a class of approximations used previously by Madden and Glandt [5] and is not consistent in this respect. The PY approximation for the fluid-fluid direct correlation function presumes that its blocking part vanishes. To get as much insight into the problem as possible, we use both closures in this work.

The inhomogeneous, or second order, Percus-Yevick (PY2) approximation implies

$$c_{b,11}(i,j)=0 \tag{8}$$

and

$$y_{ij}(1,2)=1+h_{ij}(1,2)-c_{ij}(1,2) \tag{9}$$

for $(i,j)=(1,0)$ and $(1,1)$. On the other hand, the inhomogeneous, or second order, hypernetted chain (HNC2) approximation reads

$$c_{b,11}(i,j)=\exp\{h_{b,11}(i,j)-c_{b,11}(i,j)\}-1-\{h_{b,11}(i,j)-c_{b,11}(i,j)\} \tag{10}$$

for the blocking term of the fluid-fluid function, and

$$y_{ij}(1,2)=\exp\{h_{ij}(1,2)-c_{ij}(1,2)\} \tag{11}$$

for $(i,j)=(1,0)$ and $(1,1)$.

Before discussing our numerical scheme, we make some preliminary comments. First, the matrix structure is evaluated from Eqs. (2)–(4). Next, we must solve Eqs. (5)–(7) either with PY2 closure for the inhomogeneous replica Ornstein-Zernike equations given by Eqs. (8) and (9) or with the HNC2 approximation defined by Eqs. (10) and (11). The problem comprises three equations of the OZ2 type. The symmetry $h_{10}(1,2)=h_{01}(2,1)$ is helpful in their solution. We apply the boundary condition, such that the one-particle cavity distribution function $y_1(z)$, $y_1(z)=\rho_1(z)\exp[\beta U(z)]$, tends to its limiting value, determined by the configurational part of the fluid chemical potential. Now let us discuss some technical aspects of the solution briefly. They are similar to those used previously [28,29]. The numerical algorithm for the solution of the IROZ equations, together with the BGY equation, and with the PY2 or HNC2 closure uses an expansion of the two-particle functions into a Fourier-Bessel series. The threefold integrations in the system of IROZ equations reduce to sums of one-dimensional integrations. In our calculations, the grid size in the normal direction has been $\Delta z=0.05$ and 121 terms in the Fourier-Bessel expansion have been included. The BGY equation contains the delta function due to the derivative of the pair interactions. Therefore the integrals in Eqs. (6) and (7) are onefold and contain the ''contact'' values of the functions $g_{ij}(z_1,z_2,\sqrt{R^2+z_{12}^2}$

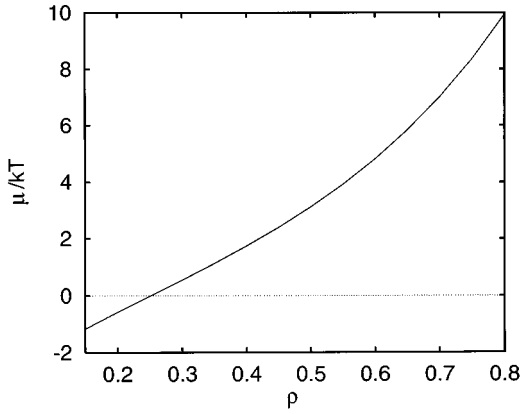

FIG. 1. Chemical potential, including ln ρ, of hard spheres as a function of the density as given by the Carnahan-Starling equation of state.

$=1$) for $(i,j)=(1,0)$ and $(1,1)$; these values have been evaluated by interpolation. As is often the case, the convergence of the numerical scheme is more difficult for the HNC2 closure than for the PY2 closure.

Finally, we discuss the methodology of the GCMC simulations for inhomogeneous quenched-annealed systems. A rectangular simulational cell whose dimensions were $10\sigma_0\times10\sigma_0\times H$ with periodic boundary conditions in the plane parallel to the pore walls was used. The simulations consisted of two steps. In the first step, the grand canonical ensemble technique was used to fill the pore with the hard sphere matrix. After equilibration, a configuration of matrix particles whose number of particles corresponded to the average number of particles at the given chemical potential was selected and the second step of the simulations was started. During this step, we performed grand canonical ensemble simulations of the fluid in a pore filled with the matrix species. At the given values of the matrix and fluid chemical potentials, the simulations were repeated several times starting from different matrix configurations. During the production runs we performed at least 5×10^6 Monte Carlo steps; each step consisted of an attempt to move, an attempt to destroy, and an attempt to create a particle that had been selected with equal probability.

We found that 5–10 replicas of the matrix usually assured good statistics for the determination of the local fluid density. However, the evaluation of the nonuniform pair distribution functions required much longer runs; at least 100 matrix replicas were necessary to calculate the correlation functions for particles parallel to the pore walls. However, even as many as 500 replicas did not ensure the convergence of the simulational results for perpendicular configurations. For this reason we do not present such results here. Comparisons with theory are made only for the configurations that are parallel to the pore walls.

III. RESULTS

Since we use the grand canonical ensemble, we give a plot of the relation between the chemical potential and density for hard spheres in Fig. 1. The approximate but quite accurate Carnahan-Starling equation of state for hard spheres was used to obtain Fig. 1.

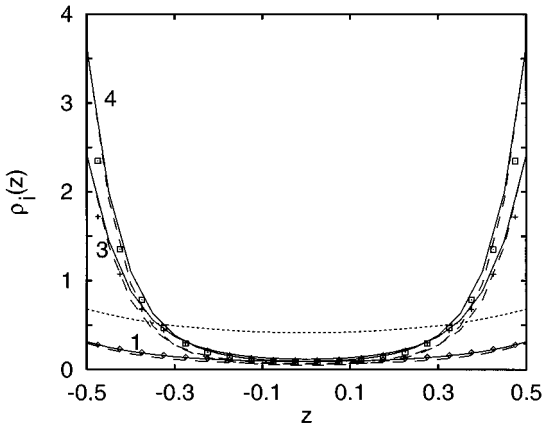

FIG. 2. A comparison of the simulated (GCMC) and theoretical (ROZ2+BGY+HNC2 and PY2 approximations) density profiles, $\rho_1(z)$, of an adsorbed fluid and in a disordered inhomogeneous matrix in a slitlike pore of the width $H=2$. The chemical potential of the matrix particles is $\beta\mu_0=0.935$. The curves labeled 1, 2, 3, and 4 here and below are for the chemical potential of fluid species $\beta\mu_1=0.935$, 3.1136, 4.8147, and 5.8346, respectively. The PY2, HNC2, and Monte Carlo results are given by the solid and dashed lines, and the symbols, respectively. The results for the state labeled 2 are not shown in this figure. The dotted line corresponds to the density profile of fixed obstacles, $\rho_0(z)$.

First, we analyze the density profiles of adsorbed fluid in matrix-filled pores at different conditions (Figs. 2–4). Figure 2 shows the density profiles obtained for $\beta\mu_0=0.935$. The density of the quenched component in a narrow pore, $H=2$, is much higher throughout the pore than is the density of its bulk counterpart. However, the matrix density distribution, $\rho_0(z)$, is almost uniform, the contact value is not much higher than in the pore center (Fig. 2). Therefore, the distribution of empty space throughout the pore width is almost homogeneous. The annealed fluid distribution is similar to that in a matrix-empty pore. At a low value for the chemical potential, $\beta\mu_1$, the presence of matrix species in this narrow pore results in a low adsorption of the annealed species. With increasing chemical potential of fluid species, the density of

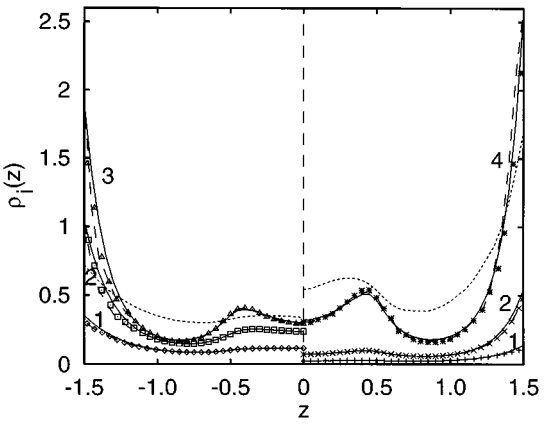

FIG. 3. The same as in Fig. 2 but for the pore $H=4$. In the left panel the chemical potential of matrix species is $\beta\mu_0=0.935$, in the right $\beta\mu_0=3.1136$. The nomenclature of the curves is similar to that in Fig. 1. The dotted line shows the matrix density profile.

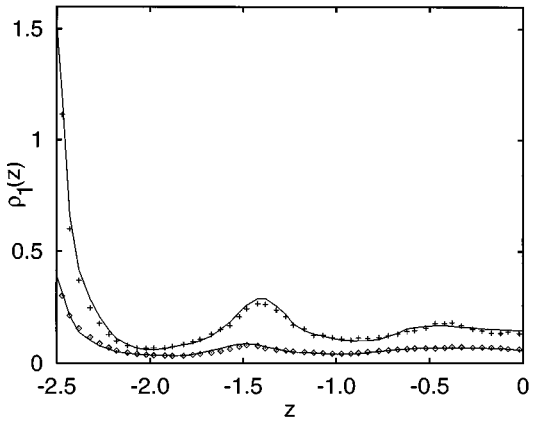

FIG. 4. The HNC2 and GCMC results for the density profiles for the case of a wide pore, $H=6$. The chemical potential of the matrix species is $\beta\mu_0=4.8147$; the chemical potential of the fluid species is $\beta\mu_1=3.1136$ (lower curves and symbols) and $\beta\mu_1=7.0026$ (upper curve and symbols).

adsorbed fluid close to the pore walls increases substantially, whereas in the pore center $\rho_1(z)$ remains almost unaltered. Both theories, namely, the HNC2 and PY2 approximations, yield very similar results for the density profiles; they both agree quite well with the computer simulation data. However, some discrepancies between the theory and simulations are observed close to the walls in a narrow pore.

Now consider adsorption in wider pores, $H=4$ (Fig. 3) and $H=6$ (Fig. 4). We have studied a fluid distribution in a pore $H=4$ at two values of the chemical potential for the quenched component, $\beta\mu_0=0.935$ and $\beta\mu_0=3.1136$. At higher $\beta\mu_0$, a more structured density profile of the matrix species is seen. In this pore, we observe layering of the adsorbed fluid at high values of the chemical potential, $\beta\mu_1$. This layering is similar to the case of a matrix-empty pore. The maxima of the density profile $\rho_1(z)$ are observed at distances that correspond to the diameter of fluid particles. It seems that the effects of adsorption of fluid species on matrix particles are not important in the model of equal diameters. With an increase of the fluid chemical potential, the pore filling occurs primarily at pore walls (Fig. 3). In the case of a wide pore, a second maximum on the density profile $\rho_1(z)$ is observed. The theory reproduces the computer simulation results quite well. The absence of a large difference between the PY2 and HNC2 theories indicates that blocking effects due to the presence of the matrix are not essential.

In Fig. 5 we show the GCMC results for the matrix density profile $\rho_0(z)$ [part (a)] for the fluid distribution in a matrix-empty pore [part (b)] and the profiles $\rho_1(z)$ in a matrix-filled pore [part (c)] for pores of various width. The contact value of $\rho_0(z)$ corresponds to a solvation force for the matrix species at the conditions before they have been quenched. The contact value of the density profile of fluid species corresponds to a solvation force of pure fluid. Because of the choice of the matrix and fluid chemical potentials (see the caption for Fig. 5) the solvation force that follows from $\rho_1(z)$ exhibits large oscillations. The contact value of the fluid particles in a matrix-filled pore does not lead to a straightforward interpretation in terms of the solvation force. We merely state that the contact values for the

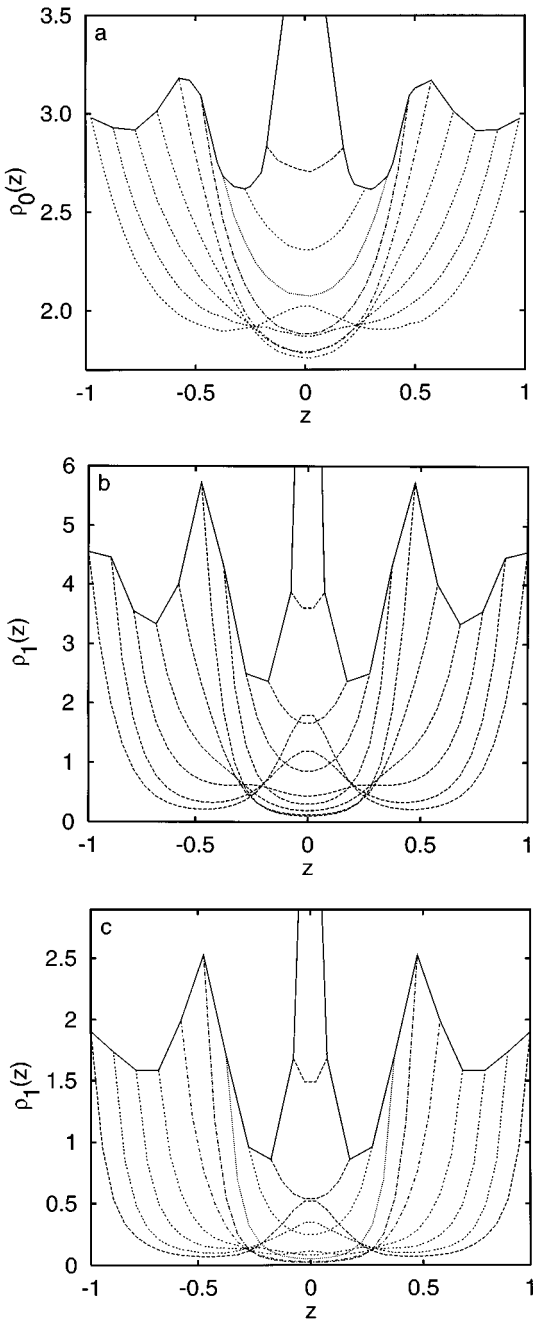

FIG. 5. (a) (solely for a matrix filled pore) The density profiles of the matrix species from the GCMC simulations for pores of different widths at a fixed value of the chemical potential $\beta\mu_0=3.1136$. The curves from left to the center are for $H=3$, 2.8, 2.6, 2.4, 2.2, 2.0, 1.8, 1.6, 1.4, and 1.2, respectively. The solid curve shows the evolution of the contact value of the density profile with pore width. (b) (solely for a fluid filled pore) The density profiles for the fluid species at the chemical potential $\beta\mu_1=8.3530$. (c) (the adsorption of the fluid in a matrix filled pore) The values of the chemical potentials for matrix and fluid species are the same as in parts (a) and (b), respectively.

profile $\rho_1(z)$ are much lower for a matrix-filled pore than for a matrix-empty pore, reflecting lower adsorption in the former case. We stress that the HNC2 approximation reproduces well the computer simulation data for pores of different widths. However, in the pore center we observe a dis-

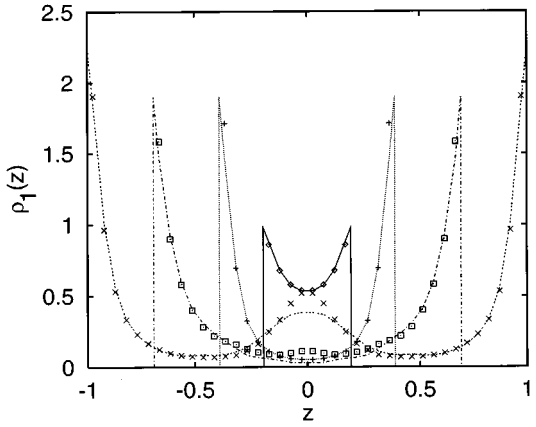

FIG. 6. A comparison of the GCMC (symbols) and HNC2 (lines) results for the density profiles of the fluid species in a matrix-filled pore. The chemical potentials of the matrix and fluid species are the same as in Fig. 5. The pore width is $H=3.0$, 2.4, 1.8, and 1.4 from left to the center.

crepancy between the theory and simulations for wide pores (Fig. 6).

The adequacy of the HNC2 approximation is not restricted to the model with equal diameters. In Fig. 7 we present a comparison between the HNC2 and GCMC results for the model in which matrix particles are two times larger than fluid particles. Again the agreement is quite good.

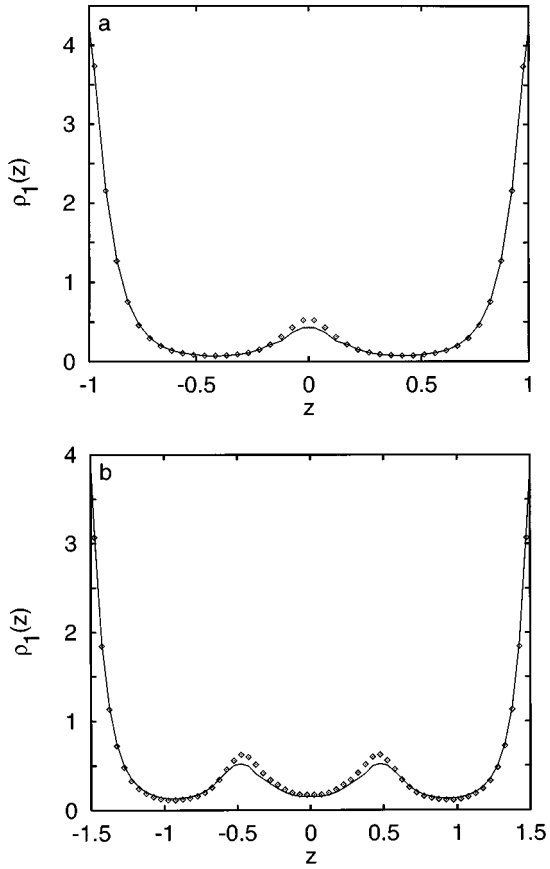

FIG. 7. A comparison of the density profiles for the adsorbed fluid species in a matrix-filled pore from GCMC simulations (symbols) and HNC2 results (solid lines) for pore width $H=3$ [part (a)] and $H=4$ [part (b)]. The diameter of the matrix particles is twice the diameter of the fluid particles. The chemical potentials of the matrix and fluid species are the same as in Fig. 5.

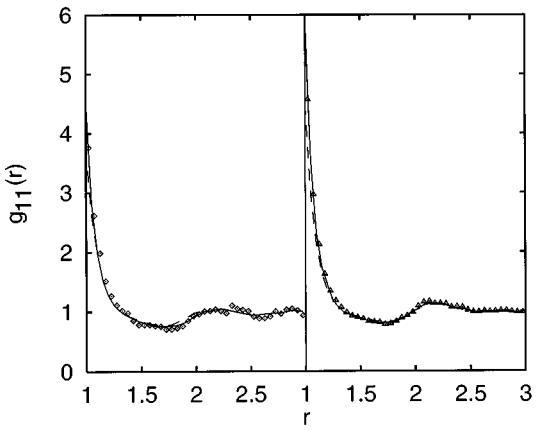

FIG. 8. A comparison of the fluid-fluid inhomogeneous pair distribution functions $g_{11}(1,2)$ obtained using the HNC2 and PY2 approximations in the ROZ2+BGY equations, with GCMC results. The functions $g_{11}^{\parallel,w}$ (left panel) and $g_{11}^{\parallel,c}$ (right panel) are for the fluid particles in a parallel configuration in the plane of closest approach to the pore walls and in the pore center. The HNC2 and PY2 results are given by the solid and dashed lines, respectively. The GCMC results are given as symbols. The fluid and matrix particles are of equal size. The chemical potentials of matrix and fluid species are as in Fig. 5. The pore width is $H=3$.

Let us proceed with a brief description of the inhomogeneous pair correlation functions for the model. Obviously, the determination of the pair correlation functions from the computer simulations is a rather difficult task for this model. In Figs. 8 and 9 we present the projections of the pair correlation functions for particles parallel to the pore walls. Those are discussed in the plane of the closest approach to the pore walls and in the pore center. In the case $H=3$, we observe that parallel correlations between the fluid particles are stronger in the pore center than at the pore walls (Fig. 8). In contrast, the fluid-matrix parallel correlations are slightly stronger in the plane of the closest approach, due to the higher value of the matrix density at the walls. The theoretical approximations (HNC2 and PY2) agree well with the

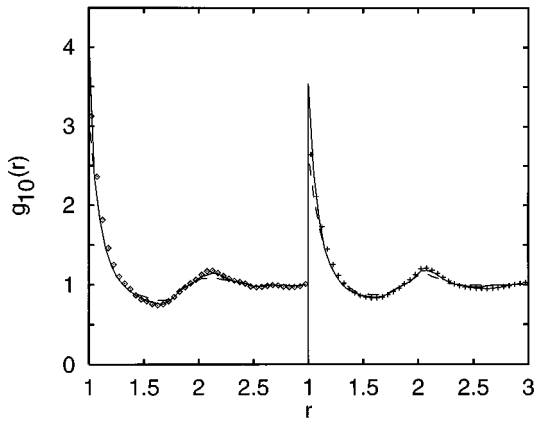

FIG. 9. The same as in Fig. 8 but for the fluid-matrix inhomogeneous pair distribution function.

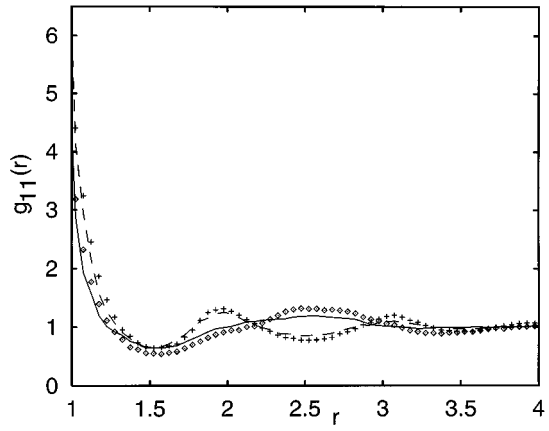

FIG. 10. The HNC2 (lines) and GCMC (symbols) fluid-fluid inhomogeneous pair distribution functions for a configuration parallel to the wall in the plane of closest approach (solid line and diamonds) and in the pore center (dashed line and crosses); $g_{11}^{\|,w}$ and $g_{11}^{\|,c}$, respectively. The diameter of matrix particles is twice the diameter of fluid particles. The chemical potentials of matrix and fluid species are as in Fig. 7. The pore width is $H=4$.

simulation data. Similarly to the case of homogeneous partly quenched systems [14], the HNC2 approximation yields slightly higher contact values for the pair correlation functions at the contact than does the PY2 approximation. The accuracy of each approximation depends on the quench conditions and on the chemical potential of fluid species. However, both theories are adequate for the model with equal diameters of particles as well as for the model when the obstacle diameter is two times larger than that of the fluid particles (Figs. 10 and 11). The discrepancy between the theories and simulations increases slightly for the model of unequal diameters in comparison with that for equal diameters, especially for intermediate interparticle separations. The positions of the second maxima of the correlation functions can be explained from geometrical considerations.

We present both the normal and parallel projections of the fluid-fluid pair correlation function in Fig. 12. It is important to note that the normal correlations are stronger in comparison to the parallel ones for small separations between fluid

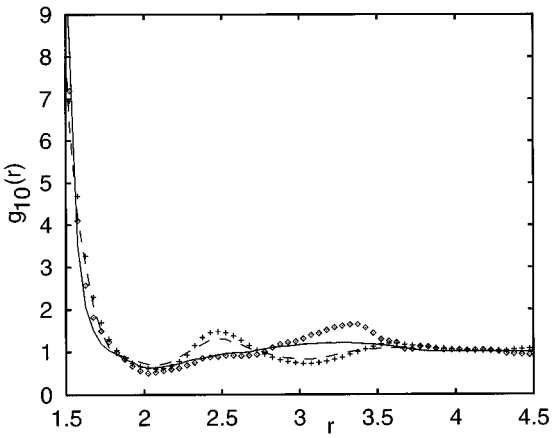

FIG. 11. The same as in Fig. 10 but for the fluid-matrix pair distribution function.

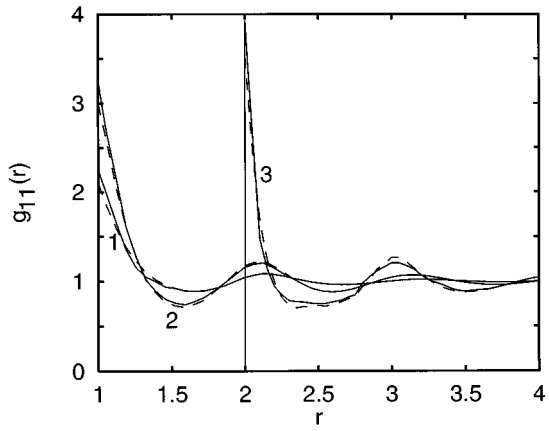

FIG. 12. The HNC2 (solid lines) and PY2 (dashed lines) inhomogeneous fluid-fluid pair distribution functions for the model with equal diameters of the fluid and matrix particles in the pore $H=4$. The chemical potentials of matrix and fluid species are $\beta\dot{\mu}_0 = 3.1136$ and $\beta\mu_1 = 5.8346$, respectively. The curves labeled 1, 2, and 3 correspond to a parallel configuration of the fluid particles in the plane of closest approach to the pore walls, in the pore center, and g_{11}^{norm}. In the normal configuration one of the fluid particles is fixed at contact with a pore wall and the second one moves along the normal to the pore wall. The pair distribution function for the normal configuration is shifted by unity along the r axis for the sake of better visualization.

particles. However, the intracore blocking effects are larger for parallel configurations of particles. Outside the hard core region, the blocking effects are negligible for all the configurations considered (Fig. 13). Similar effects to those shown in Fig. 12 are observed for the fluid-matrix pair correlation function (Fig. 14).

IV. CONCLUSIONS

We have solved the inhomogeneous replica OZ equations for a model of an inhomogeneously quenched matrix and an inhomogeneous fluid. We have considered the simplest model (hard spheres) and approximations. When the pore is wide, ''layering'' is found in the density profiles. As the pore becomes more narrow, these layers are ''squeezed'' out. The

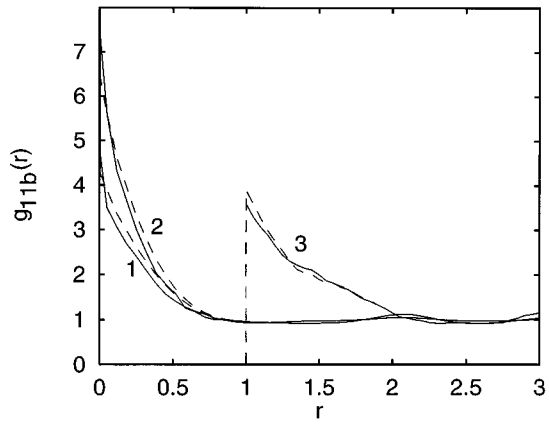

FIG. 13. The blocking parts of the inhomogeneous pair distribution functions for fluid particles given in Fig. 12 under all the same conditions.

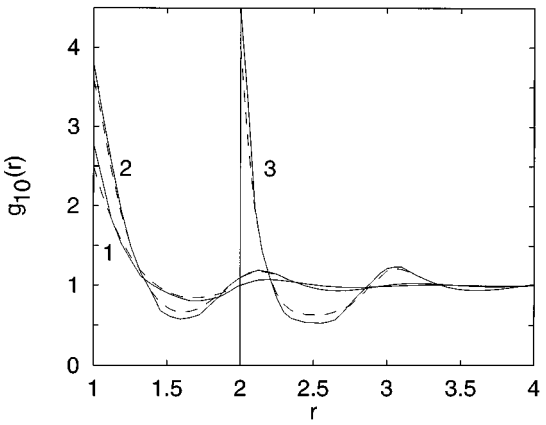

FIG. 14. The same as in Fig. 12 but for the inhomogeneous fluid-matrix pair distribution function.

profiles are large near the pore walls and smaller near the center of the pore. When the pore becomes very small, the value of the profile at the center becomes larger so that the profile is nearly uniform. Both the PY and HNC approximations lead to good agreement with our GCMC simulation results. In addition, we have reported some results for the pair correlation functions.

If more sophisticated approximations for the IROZ equations were used (the hypernetted chain closure consistent with the ROZ equations may be implemented without difficulty) and models that include more complex and attractive fluid-fluid, fluid-matrix, and fluid-walls interactions were used, we expect that interesting effects (such as phase transitions) would be found. The question of the accuracy of the PY and HNC approximations should be reconsidered in these situations. Density functional theory should be considered. So far, such theories have not been applied to inhomogeneous partly quenched systems. Also, interesting possibilities can arise if the matrix would be prepared in some special way.

Undoubtedly, these and other options may yield unexpected and rich structural and thermodynamic behavior in partly quenched confined systems. The perspectives for investigations in the field that is just opened by the solution of IROZ equations are very promising.

ACKNOWLEDGMENTS

This work has been supported by the U.S. National Science Foundation (Grant No. CHE96-01971), the donors of the Petroleum Research Fund administered by the American Chemical Society (Grant No. ACS-PRF-31573-AC9), and by Silicon Graphics, Inc.—Cray Research of Mexico under one of its university research and development grants. D.H. would like to thank the John Simon Guggenheim Memorial Foundation for financial support. Valuable discussions with A. Patrykiejew are gratefully acknowledged. A. K., D. H., and O. P. are grateful to the Faculty of Chemistry of the Marie Curie Sklodowska University for its hospitality and partial support during their visits to Lublin.

[1] B. J. Frisken and D. S. Cannell, Phys. Rev. Lett. **69**, 632 (1992).
[2] M. C. Goh, W. I. Goldburg, and C. M. Knobler, Phys. Rev. Lett. **58**, 1008 (1987).
[3] A. P. Y. Wong, S. B. Kim, W. I. Goldburg, and M. H. W. Chan, Phys. Rev. Lett. **70**, 954 (1993).
[4] S. B. Dierker and P. Wiltzius, Phys. Rev. Lett. **66**, 1185 (1991).
[5] W. G. Madden and E. D. Glandt, J. Stat. Phys. **51**, 537 (1988).
[6] W. G. Madden, J. Chem. Phys. **96**, 5422 (1992).
[7] J. A. Given and G. Stell, Physica A **209**, 495 (1994).
[8] J. A. Given and G. Stell, in *Proceedings of the XVIth International Workshop on Condensed Matter Theories*, edited by L. Blum and F. B. Malik (Plenum, New York, 1993).
[9] J. A. Given and G. Stell, J. Chem. Phys. **97**, 4573 (1992).
[10] E. Pitard, M. L. Rosinberg, G. Stell, and G. Tarjus, Phys. Rev. Lett. **74**, 4361 (1995).
[11] C. Vega, R. D. Kaminsky, and P. A. Monson, J. Chem. Phys. **99**, 3003 (1993).
[12] K. S. Page and P. A. Monson, Phys. Rev. E **54**, R29 (1996).
[13] M. L. Rosinberg, G. Tarjus, and G. Stell, J. Chem. Phys. **100**, 5172 (1994).
[14] E. Lomba, J. A. Given, G. Stell, J. J. Weis, and D. Levesque, Phys. Rev. E **48**, 233 (1993).
[15] A. Meroni, D. Levesque, and J. J. Weis, J. Chem. Phys. **105**, 1101 (1996).
[16] D. M. Ford and E. D. Glandt, Phys. Rev. E **50**, 1280 (1994).
[17] D. M. Ford and E. D. Glandt, J. Chem. Phys. **100**, 2391 (1994).
[18] J. Given, J. Chem. Phys. **102**, 2934 (1995).
[19] E. Kierlik, M. L. Rosinberg, G. Tarjus, and P. A. Monson, J. Chem. Phys. **106**, 264 (1997).
[20] D. Bratko and A. Chakraborty, Phys. Rev. E **50**, 218 (1994).
[21] D. Bratko and A. Chakraborty, J. Chem. Phys. **105**, 7700 (1995).
[22] D. Henderson, A. Patrykiejew, O. Pizio, and S. Sokołowski, Physica A **233**, 67 (1996).
[23] A. Trokhymchuk, O. Pizio, M. Holovko, and S. Sokołowski, J. Phys. Chem. **100**, 17004 (1996).
[24] A. Trokhymchuk, O. Pizio, M. Holovko, and S. Sokołowski, J. Chem. Phys. **106**, 200 (1997).
[25] O. Pizio, A. Trokhymchuk, S. Labik, and D. Henderson, J. Colloid Interface Sci. **191**, 86 (1997).
[26] W. Dong, E. Kierlik, and M. L. Rosinberg, Phys. Rev. E **50**, 4750 (1994).
[27] O. Pizio and S. Sokołowski, Phys. Rev. E **56**, 63 (1997).
[28] S. Sokołowski, J. Chem. Phys. **73**, 3507 (1980).
[29] D. Henderson, S. Sokołowski, and D. T. Wasan, J. Stat. Phys. **89**, 233 (1997).